

# Fluorescence quenching by polystyrene microspheres in UV-visible and NIR tissue-simulating phantoms

Karthik Vishwanath, Wei Zhong, Melanie Close, and Mary-Ann Mycek\*

*Department of Biomedical Engineering, University of Michigan  
2200 Bonisteel Blvd., Ann Arbor, MI 48109-2099 USA  
[mycek@umich.edu](mailto:mycek@umich.edu)*

**Abstract:** Tissue-simulating phantoms are widely used for controlled studies of photon transport in turbid media. Here, we describe how polystyrene microspheres, which are often used to simulate optical scattering in such phantoms, can reduce fluorophore quantum yield via collisional quenching. We report studies on UV-visible (fluorescein-based) and NIR (IR125-based) phantoms with differing fluorophore and scatterer concentrations, as well as differing microsphere sizes. Results consistent with the Stern-Volmer relation suggest that the fluorophore intrinsic excited-state lifetime decreased due to collisional quenching from polystyrene microspheres and that the quenching efficiency was dependent on the concentration ratio of fluorophores to microspheres. Lifetime decreases ranging from 10-35% (20%) were measured for fluorescein-based (IR 125-based) phantoms. Since polystyrene microspheres are commonly used in tissue-simulating phantoms for quantitative studies of fluorescence light propagation, their quenching effects on fluorescence intensities may be difficult to separate from intensity losses attributed to optical absorption and scattering in the phantom unless fluorescence lifetime measurements are performed simultaneously.

©2006 Optical Society of America

**OCIS codes:** (170.3650) Lifetime-based sensing; (170.7050) Turbid media; (170.6280) Spectroscopy, fluorescence and luminescence; (999.9999) Tissue-simulating phantoms

---

## References and links

1. R. F. Mould, ed. Medical Science Series (IOP Publishing Ltd, London, 1988).
2. D. J. Dowsett, P. A. Kenny, and R. E. Johnston, The physics of Diagnostic imaging (Chapman & Hall, London, 1998).
3. D. F. Jackson, ed. Progress in medical and environmental physics (Surrey University Press, London, 1982).
4. J. V. Hajnal, and G. M. Bydder, "Registration and subtraction of serial magnetic resonance images Part 1: Technique," in Advanced MR imaging techniques, W. G. J. Bradley, and G. M. Bydder, eds. (Martin Dunitz Ltd, London, 1997), pp. 221-237.
5. J. C. Hebden, D. J. Hall, M. Firbank, and D. T. Delpy, "Time-resolved optical imaging of a solid tissue-equivalent phantom." *Appl. Opt.* **34**, 8038-8047 (1995).
6. K. Rinzema, L. H. P. Murrer, and W. M. Star, "Direct experimental verification of light transport theory in an optical phantom." *J. Opt. Soc. Am. A* **15**, 2078-2088 (1998).
7. A. Sefkow, M. Bree, and M.-A. Mycek, "A method for measuring cellular optical absorption and scattering evaluated using dilute cell suspension phantoms." *Appl. Spectrosc.* **55**, 1495-1501 (2001).
8. A. J. Durkin, S. Jaikumar, and R. Richards-Kortum, "Optically dilute, absorbing, and turbid phantoms for fluorescence spectroscopy of homogeneous and inhomogeneous samples." *Appl. Spectrosc.* **47**, 2114-2121 (1993).
9. A. B. Milstein, S. Oh, K. J. Webb, C. A. Bouman, Q. Zhang, D. A. Boas, and R. P. Millane, "Fluorescence optical diffusion tomography." *Appl. Opt.* **42**, 3081-3094 (2003).

10. K. Vishwanath, B. W. Pogue, and M.-A. Mycek, "Quantitative fluorescence lifetime spectroscopy in turbid media: comparison of theoretical, experimental and computational methods." *Phys. Med. Biol.* **47**, 3387-3405 (2002).
11. H. Jiang, S. Ramesh, and M. Bartlett, "Combined Optical and Fluorescence Imaging for Breast Cancer Detection and Diagnosis." *Crit. Rev. Biomed. Eng.* **28**, 371-375 (2000).
12. E. M. Sevick-Muraca, G. Lopez, J. S. Reynolds, T. L. Troy, and C. Hutchinson, "Fluorescence and absorption contrast mechanisms for biomedical optical imaging using frequency-domain techniques." *Photochem. Photobiol.* **66**, 55-64 (1997).
13. T. J. Pfefer, L. S. Matchette, A. M. Ross, and M. N. Ediger, "Selective detection of fluorophore layers in turbid media: the role of fiber-optic probe design." *Opt. Lett.* **28**, 120-122 (2003).
14. A. Thompson, and E. M. Sevick-Muraca, "Near-infrared fluorescence contrast-enhanced imaging with intensified charge-coupled device homodyne detection: measurement precision and accuracy." *J. Biomed. Opt.* **8**, 111-120 (2003).
15. A. E. Cerussi, J. S. Maier, S. Fantini, M. A. Franceschini, W. W. Mantulin, and E. Gratton, "Experimental verification of a theory for the time-resolved fluorescence spectroscopy of thick tissues." *Appl. Opt.* **36**, 116-124 (1997).
16. S. Flock, B. Wilson, and M. Patterson, "Monte Carlo modeling of light propagation in highly scattering tissues-II: Comparison with measurements in phantoms." *IEEE Transactions on Biomedical Engineering* **36**, 1169-1173 (1989).
17. J. R. Mourant, T. Fuselier, J. Boyer, T. Johnson, and I. Bigio, "Predictions and measurements of scattering and absorption over broad wavelength ranges in tissue phantoms." *Appl. Opt.* **36**, 949-957 (1997).
18. B. B. Das, L. Feng, and R. R. Alfano, "Time-resolved fluorescence and photon migration studies in biomedical and model random media." *Rep. Prog. Phys.* **60**, 227-292 (1997).
19. A. Kienle, and M. S. Patterson, "Determination of the optical properties of semi-infinite turbid media from frequency-domain reflectance close to the source." *Phys. Med. Biol.* **42**, 1801-1819 (1997).
20. M. Patterson, B. Chance, and B. Wilson, "Time resolved reflectance and transmittance for the non-invasive measurement of tissue optical properties." *Appl. Opt.* **28**, 2331-2336 (1989).
21. E. M. Sevick-Muraca, J. S. Reynolds, T. L. Troy, G. Lopez, and D. Y. Paithankar, "Fluorescence lifetime spectroscopic imaging with measurements of photon migration," in *Advances in Optical Biopsy and Optical Mammography*, (1998), pp. 46-57.
22. R. K. Wang, and Y. A. Wickramasinghe, "Fast algorithm to determine optical properties of a turbid medium from time-resolved measurements." *Appl. Opt.* **37**, 7342-7351 (1998).
23. S. A. Ramakrishna, and K. D. Rao, "Estimation of light transport parameters in biological media using coherent backscattering." *Pramana, J. Phys.* **54**, 255-267 (2000).
24. M. S. Nair, N. Ghosh, N. S. Raju, and A. Pradhan, "Determination of optical parameters of human breast tissue from spatially resolved fluorescence: a diffusion theory model." *Appl. Opt.* **41**, 4024-4035 (2002).
25. N. Ramanujam, "Fluorescence spectroscopy of neoplastic and non-neoplastic tissues." *Neoplasia* **2**, 89-117 (2000).
26. S. J. Madsen, M. S. Patterson, and B. C. Wilson, "The use of India ink as an optical absorber in tissue-stimulating phantoms." *Phys. Med. Biol.* **37**, 985-993 (1992).
27. S. Flock, S. L. Jacques, B. C. Wilson, W. Star, and M. Van Gemert, "Optical properties of Intralipid: A phantom medium for light propagation studies." *Lasers in Surgery and Medicine* **12**, 510-519 (1992).
28. C. L. Hutchinson, T. L. Troy, and E. M. Sevickmuraca, "Fluorescence-lifetime determination in tissues or other scattering media from measurement of excitation and emission kinetics." *Appl. Opt.* **35**, 2325-2332 (1996).
29. T. Farrell, M. Patterson, and M. Essenpreis, "Influence of layered tissue architecture on estimates of tissue optical properties obtained from spatially resolved diffuse reflectometry." *Appl. Opt.* **37**, 1958-1972 (1998).
30. J. R. Mourant, I. J. Bigio, D. A. Jack, T. M. Johnson, and H. D. Miller, "Measuring absorption coefficients in small volumes of highly scattering media: source detector separations for which path lengths do not depend on scattering properties." *Appl. Phys.* **36**, 5655 - 5661 (1997).
31. D. Y. Paithankar, A. U. Chen, B. W. Pogue, M. S. Patterson, and E. M. Sevickmuraca, "Imaging of fluorescent yield and lifetime from multiply scattered light reemitted from random media." *Appl. Opt.* **36**, 2260-2272 (1997).
32. M. S. Patterson, and B. W. Pogue, "Mathematical model for time-resolved and frequency-domain fluorescence spectroscopy in biological tissues." *Appl. Opt.* **33**, 1963-1974 (1994).
33. L. Wang, D. Liu, N. He, S. L. Jacques, and S. L. Thomsen, "Biological laser action." *Appl. Opt.* **35**, 1775-1779 (1996).
34. E. M. Sevick-Muraca, A. Godavarty, J. P. Houston, A. B. Thompson, and R. Roy, "Near-infrared imaging with fluorescent contrast agents," in *Handbook of Biomedical Fluorescence*, M.-A. Mycek, and B. W. Pogue, eds. (Marcel-Dekker Inc., New York, New York, 2003), pp. 445-527.

35. G. Wagnieres, S. Cheng, M. Zellweger, N. Utke, D. Braichotte, J.-P. Ballini, and H. Van Den Bergh, "An optical phantom with tissue-like properties in the visible for use in PDT and fluorescence spectroscopy." *Phys. Med. Biol.* **42**, 1415-1426 (1997).
36. K. Vishwanath, and M.-A. Mycek, "Time-resolved photon migration in bi-layered tissue models." *Optics Express* **13**, 7466-7482 (2005).
37. K. Vishwanath, and M.-A. Mycek, "Polystyrene microspheres in tissue-simulating phantoms can collisionally quench fluorescence." *J. Fluorescence* **13**, 105-108 (2003).
38. J. R. Lakowicz, *Principles of Fluorescence Spectroscopy* (Kluwer Academic/Plenum, New York, 1999).
39. J. S. Reynolds, T. L. Troy, R. H. Mayer, A. B. Thompson, D. J. Waters, K. K. Cornell, P. W. Snyder, and E. M. Sevick-Muraca, "Imaging of spontaneous canine mammary tumors using fluorescent contrast agents." *Photochem. Photobiol.* **70**, 87-94 (1999).
40. N. Ramanujam, G. Vishnoi, A. Hielscher, M. Rode, I. Forouzan, and B. Chance, "Photon migration through fetal head in utero using continuous wave, near infrared spectroscopy: clinical and experimental model studies." *J. Biomed. Opt.* **5**, 173-184 (2000).
41. J. D. Pitts, and M.-A. Mycek, "Design and development of a rapid acquisition laser-based fluorometer with simultaneous spectral and temporal resolution." *Review of Scientific Instruments* **72**, 3061-3072 (2001).
42. H. C. Van De Hulst, *Light Scattering by Small Particles* (Wiley and Sons, New York, 1957).
43. W.-F. Cheong, S. Prah, and S. Welch, "A review of the optical properties of biological tissues." *IEEE J. Quantum Electron.* **26**, 2166-2185 (1990).
44. Z. S. Kolber, and M. D. Barkley, "Comparison of approaches to the instrument response function in fluorescence decay measurements." *Anal. Biochem.* **152**, 6-21 (1986).
45. K. R. Diamond, T. J. Farrell, and M. S. Patterson, "Measurement of fluorophore concentrations and fluorescence quantum yield in tissue-simulating phantoms using three diffusion models of steady-state spatially resolved fluorescence." *Phys. Med. Biol.* **48**, 4135-4149 (2003).
46. D. Stasic, T. J. Farrell, and M. S. Patterson, "The use of spatially resolved fluorescence and reflectance to determine interface depth in layered fluorophore distributions." *Phys. Med. Biol.* **48**, 3459-3474 (2003).

## 1. Introduction

Tissue-simulating phantoms are artificial materials widely used in medical imaging and spectroscopy studies, because they are designed to replicate the interactions of biological tissues with physical probes, such as ionizing radiation, ultrasound, radio-frequency waves, magnetic fields, and laser light [1-4]. Phantoms represent reproducible standards that can be employed for the quantitative assessment of such physical methods, for purposes of instrument calibration, detection sensitivity demonstration in spectroscopy, and resolution and contrast determination in imaging [1-4].

In biomedical optics, phantoms have been designed to simulate tissues with varying optical properties (e.g., optical absorption  $\mu_a$  and scattering coefficients  $\mu_s$ ) [5-7], fluorescence properties (e.g., excitation  $\lambda_{ex}$  and emission  $\lambda_{em}$  wavelengths, fluorophore quantum yield  $\Phi_f$  and excited state lifetime  $\tau_0$ ) [8-10], anthropomorphic spatial dimensions [11, 12], and spatially localized inhomogeneities [11-14]. Such phantoms have been employed successfully not only to calibrate and test biomedical optical instrumentation, but also to validate theoretical models of light propagation within turbid media [6, 7, 10, 15-25].

Materials used to create tissue-simulating phantoms for optical studies depend on the region of the electromagnetic spectrum under investigation. Commonly used absorbers in the ultraviolet (UV) – visible include India ink, methylene blue, and Evans blue dye [7, 16, 23-26], although India ink has a significant scattering component [26] and is not suitable as a pure absorber. Scatterers employed at wavelengths extending from the UV to the infrared (IR) include Intralipid, Liposyn, silicon dioxide, Latex, and polystyrene microspheres [6, 7, 14, 24, 25, 27-30]. Intralipid's variable composition and scatterer size distribution have been noted previously [7, 27], suggesting that polystyrene microspheres, with relatively uniform composition and narrow size distributions [7], would be superior as a pure scatterer. Indeed, polystyrene microspheres have been shown to be useful as pure scatterers, with negligible

absorption and fluorescence [8]. Available in a wide range of sizes comparable to scatterer sizes in biological tissues, the scattering coefficients of the spheres can be calculated from Mie theory [7, 10, 17]. Fluorophores employed in phantoms include laser dyes such as rhodamine, furan-2, and fluorescein for UV-visible excitation and emission, as well as indocyanine green (ICG), diethylthiatricarbocyanine iodide (DTTCl), IR-125, and IR-140 for studies in the near infrared (NIR) [12, 21, 31-34]. To create tissue phantoms with homogeneous optical properties, independently controlled mixtures of pure absorbing, scattering, and fluorescing components can be fabricated using, e.g., deionized water for liquid solutions or agarose gel for solid forms [5, 8, 35]. Inhomogeneities are frequently introduced to simulate tumors embedded in normal tissues or layers [12] of epithelial tissues [11, 13, 36].

In constructing such tissue-simulating phantoms, it is ideal to employ materials that will act reproducibly as “pure” optical absorbers or scatterers, and, further, will remain unaffected by the presence of other phantom components. (Known limitations to India ink and Intralipid have been noted above.) Likewise, in fluorescent phantoms, fluorophores should retain their optical properties ( $\lambda_{ex}$ ,  $\lambda_{em}$ ,  $\Phi_{fl}$ ,  $\tau_0$ ) independent of optical absorption and scattering coefficients in the phantom. A preliminary study revealed that using 1  $\mu\text{m}$  diameter polystyrene microspheres to provide optical scattering ( $\mu_s = 100 - 600 \text{ cm}^{-1}$ ) in a tissue phantom containing fluorescein dye reduced the quantum yield of the fluorophore via collisional quenching [37], prompting the extended studies reported here. Fluorescence quenching, in general, refers to any physical mechanism causing a decrease in measured fluorescence intensity [38]. Collisional quenching refers to the decrease in fluorophore quantum yield  $\Phi_{fl}$  (the ratio of emitted to absorbed photons) that occurs when an excited fluorophore returns non-radiatively to the ground state due to physical interactions (collisions) with an agent (quencher). (An example would be the well known quenching of fluorescence caused by the presence of the quencher oxygen in a sample.) In reducing the quantum yield, collisional quenching affects not only the measured fluorescence intensity ( $I$ ) relative to the value in the absence of quenching ( $I_0$ ), but also the fluorophore’s excited state lifetime ( $\tau$ ) relative to the value in the absence of quenching ( $\tau_0$ ). Mathematically, these values are related to the quencher concentration [ $Q$ ] via the Stern-Volmer equation [38].

$$\frac{I_0}{I} = \frac{\tau_0}{\tau} = 1 + K_D[Q] \quad (1)$$

where  $K_D$  is the Stern-Volmer quenching constant.

In turbid scattering samples, such as tissue phantoms, fluorescence intensity losses from collisional quenching may be difficult to distinguish and isolate from the expected intensity losses arising from optical scattering or other sources. Therefore, measurements of fluorophore lifetime are particularly useful to detect collisional quenching in these samples. (Indeed, because they are insensitive to other forms of quenching, decreases in fluorescence lifetime are considered to offer proof of the collisional quenching mechanism in a sample<sup>[38]</sup>.) The previous report employed time-domain fluorescence lifetime spectroscopy to detect a decrease of up to 17% of both the fluorophore lifetime and the remitted fluorescence intensity at a 10  $\mu\text{M}$  concentration of fluorescein in the presence of 1  $\mu\text{m}$  diameter polystyrene microspheres (quencher), in accordance with the Stern-Volmer equation (Eq. (1)) describing collisional quenching [38].

Here, we present results of time-resolved fluorescence studies in fluorescein-based tissue phantoms with varying polystyrene microsphere (quencher) concentrations and varying sizes to investigate whether the degree of collisional quenching observed is related to the total available surface area presented by the microspheres. Further, we extend these studies from the UV-visible region of the electromagnetic spectrum to the NIR, where such tissue

phantoms have been frequently employed for fluorescence optical diffusion and photon migration studies [9, 12, 14, 39, 40].

Section 2 describes the instrumentation used for time-domain fluorescence lifetime spectroscopy, the phantom preparation process, and data analysis. Section 3 reports the experimental results and discusses implications of these results to UV-visible-NIR studies that use fluorescent phantoms prepared with polystyrene microspheres to provide optical scattering.

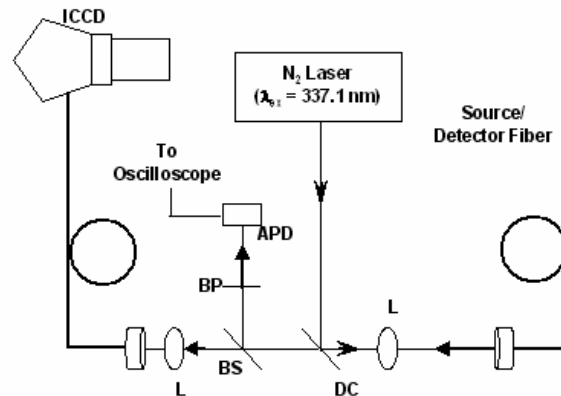


Fig. 1. Schematic of the nanosecond UV fluorescence lifetime spectrometer (UV-FLS) instrumentation used for studies at 337.1 nm excitation. ICCD- Intensified Charge Coupled Device; APD- Avalanche Photodiode; DC- Dichroic Mirror; L - Lens; BS- Beam Splitter; BP- Band Pass Filter.

## 2. Experiment

### 2.1. Instrumentation

Two fluorescence lifetime spectrometers were employed for these studies. Both were time-domain systems, one using ns laser pulses for UV excitation of fluorescein ( $\lambda_{\text{ex}} = 337.1 \text{ nm}$ ), the other using ps laser pulses for NIR excitation of IR-125 ( $\lambda_{\text{ex}} = 777 \text{ nm}$ ).

#### 2.1.1. UV Fluorescence lifetime spectrometer (UV-FLS)

Fluorescein-containing phantoms were studied using a nanosecond UV fluorescence lifetime spectrometer (UV-FLS), whose design and calibration was described previously [41]. Figure 1 shows the schematic configuration of the instrument. Briefly, the UV-FLS provided excitation light at 337.1 nm from a pulsed nitrogen laser (VSL-337, Laser Science Inc., Franklin MA; FWHM = 4 ns) that was coupled to a quartz optical fiber (600  $\mu\text{m}$  diameter, 0.22 N.A., SFS600/660N, Fiberguide Industries, Stirling, NJ) and delivered to the phantom medium by holding the distal end of the fiber just beneath the phantom surface. The remitted fluorescence was collected by the same fiber, filtered by a dichroic mirror, and split into two parts via the beam splitter. One part was coupled to an optical fiber that delivered the light to the entrance slit of a spectrograph (MS125, Oriel Instruments, Stratford, CT) equipped with a gated, intensified charged coupled device (ICCD, Andor Technology, Belfast, Northern Ireland) at the exit port. This spectrally resolved fluorescence data was employed to verify the integrity of the samples. The other part of the fluorescence was filtered via a bandpass filter centered at  $540 \pm 10 \text{ nm}$  and focused onto an avalanche photodiode (APD) (C5658, Hamamatsu, Bridgewater, NJ) with a rise time of 300 ps to

collect the dynamics of the remitted fluorescence. The transient response from the APD was digitized on a 1 GHz (5 GS/s) oscilloscope (TDS-680C, Tektronix, Wilsonville, OR) to obtain the time-resolved fluorescence decay. This data was then analyzed to extract the fluorescence lifetime  $\tau$  of the fluorophore species, as described below [10, 41].

### 2.1.2. NIR fluorescence lifetime spectrometer (NIR-FLS)

Phantoms containing IR-125 as the fluorophore were studied using a second system that employed a pulsed, picosecond nitrogen laser providing excitation at  $\lambda = 337.1$  nm (GL-3300, Photon Technology International, Lawrenceville, NJ) to pump a tunable (wavelength range 365-960 nm), pulsed dye laser (GL-301, Photon Technology International). A  $1.2 \times 10^{-3}$  M solution of DOTC-Iodide (Cat. # 08250, Exciton, Dayton, OH) in DMSO was placed into the dye laser to produce the excitation source (centered at  $\lambda_{ex} = 777$  nm; FWHM = 1.1 ns) that was then used to excite IR-125 in the phantoms. A schematic of the instrumentation is shown in Fig. 2. The excitation light was coupled into a source fiber-optic (600  $\mu$ m diameter, 0.22 N.A., SFS600/660N, Fiberguide Industries, Stirling, NJ) that was held just below the phantom surface and used to illuminate the sample. The remitted fluorescence was detected via an identical fiber, which was adjacent to the source fiber such that the fiber centers were separated by the fiber diameter (inset in Fig. 2). The remitted fluorescence decay was attenuated by a neutral density filter (03FNQ015, Melles Griot, Irvine, CA) and filtered through a band pass filter (centered at  $830 \pm 10$  nm) before being focused by a lens onto an APD (C5658, Hamamatsu), whose transient response was digitized on a 1 GHz (4 GS/s) oscilloscope (TDS-784A, Tektronix) to obtain the time-resolved fluorescence decay.

The single-fiber geometry for excitation and detection used in the UV-FLS for fluorescein phantoms was not implemented in the NIR-FLS for IR-125 phantoms, as it was not possible to obtain the appropriate dichroic to selectively reflect the excitation light at 777 nm. Although it was demonstrated previously that using multiple source-detector fiber-optic configurations could cause distortions in the measured fluorescence decay trace obtained from a fluorescent species present in a scattering medium, we note that the source-detector separation (600  $\mu$ m) maintained for the measurements reported here was sufficiently small to

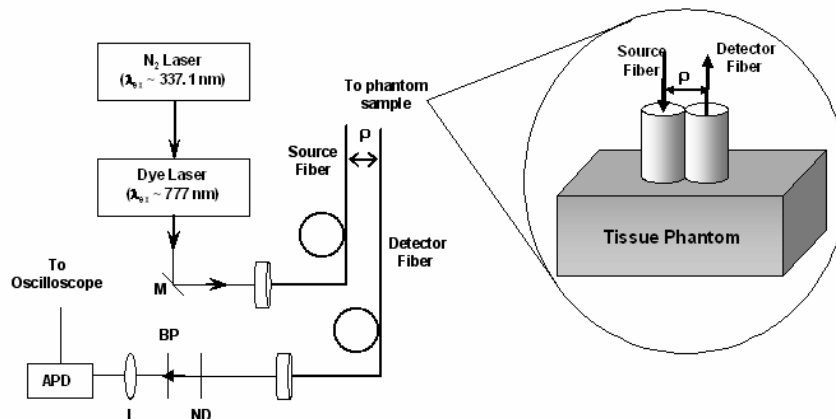


Fig. 2. Schematic of the picosecond NIR fluorescence lifetime spectrometer (NIR-FLS) instrumentation used for studies at 777 nm. APD- Avalanche Photodiode; M- Mirror; L - Lens; BS- Beam Splitter; ND- Neutral Density Filter; BP- Band Pass Filter. The inset shows the alignment of the source and detector optical fibers used for excitation and collection of fluorescent light from the sample tissue phantom.

neglect these apparent distortions (less than 1% effect) [10].

## 2.2. Phantom preparation

Phantom series were prepared with differing fluorophore concentrations and with polystyrene microspheres of varying diameters, as listed in Table 1. Fluorescein (Cat#. F6377, Sigma-Aldrich, St. Louis, MO) and IR-125 (Cat#. 09030, Exciton, Dayton, OH) dyes were used as fluorophores in the phantoms. Polystyrene microspheres with diameters 0.5  $\mu\text{m}$ , 1.0  $\mu\text{m}$  and 2.0  $\mu\text{m}$  (Cat#. 07307, 07310 and 19814, respectively, Polysciences, Warrington, PA) were used as scatterers. The fluorescein phantoms used de-ionized water (DI H<sub>2</sub>O) as the solvent, while the IR-125 phantoms used ethanol as the solvent [28].

Table 1. Phantom composition

Phantom series	Fluorescent dye	Microsphere diameter [ $\mu\text{m}$ ]	Dye concentration [ $\mu\text{M}$ ]
A	Fluorescein	2.0	40
B	Fluorescein	1.0	40
C	Fluorescein	0.5	40
D	Fluorescein	2.0	8
E	Fluorescein	1.0	8
F	Fluorescein	0.5	8
G	IR-125	2.0	1
H	IR-125	2.0	10

Phantoms were prepared in a series with scatterer (polystyrene microsphere) fractions ranging between 0% through 50% by volume (in steps of 10%) in plastic cuvettes. As shipped by the manufacturer, the microsphere suspensions contained 2.5% of polystyrene per ml by weight and this maximally concentrated suspension was termed as having 100% scatterers per unit volume or, equivalently, had volume fraction of scatterers  $f = 1$ . The first phantom prepared in a series contained no scatterers (0% polystyrene microspheres) and was prepared by diluting a concentrated ( $\sim 1$  mM) stock solution of the fluorophore to a final volume of 4 ml to obtain the desired concentration. This phantom (0% scatterers) gave the intrinsic lifetime  $\tau_0$  of the fluorophore. Half the volume (2 ml) of the phantom solution was removed from the cuvette and 2 ml of manufacturer shipped microsphere suspension was added to obtain the first phantom in the series, which contained 50% scatterers per unit volume ( $f = 0.5$ ). Since this addition of scatterers perturbed the fluorophore concentration in the phantom, a very small volume ( $\sim \mu\text{l}$ ) of the stock dye solution ( $\sim 1$  mM) was added so that the resulting fluorophore concentration was readjusted to the initial fluorophore concentration, while the scatterer concentration remained relatively unchanged. Subsequent phantoms in the series were prepared by removing a certain volume of phantom solution from the cuvette, diluting the phantom to a total volume of 4 ml with the appropriate solvent, and readjusting fluorophore concentration with the concentrated dye solution.

Each prepared phantom was measured three times at room temperature ( $\approx 20$  C). The resulting time-resolved traces were stored and analyzed as described below to extract the fluorescence lifetime  $\tau$  for every phantom in the series. We note that it was determined experimentally that the concentrations of the fluorophores used (a) were devoid of artifacts arising from reabsorption (inner filter) effects by ascertaining a linear increase in peak fluorescence signal strength with increasing fluorophore concentrations between 1-50  $\mu\text{M}$  [38] and (b) generated fluorescence signal strengths comparable to those emanating from tissue *in vivo* (verified by comparison with the fluorescence signal strength measured on the spectrometer upon holding the fiber probe flush with the experimenter's forearm) [41].

For each phantom, the extinction cross section,  $C_{\text{ext}}$ , of the microspheres was determined at the relevant wavelengths using manufacturer supplied data for the microspheres (index of

refraction of the polystyrene spheres, sphere diameters, and number density of the spheres in suspension) and the Van de Hulst approximation to Mie theory [7, 42]. It was assumed that the polystyrene microspheres were perfectly spherical non-absorbing particles[8], which equated their extinction cross sections to their scattering cross sections. The scattering coefficients of the manufacturer shipped microsphere solutions were determined by multiplying  $C_{\text{ext}}$  with  $N_s$ . Here,  $N_s$  was the microsphere density per unit volume in the suspension, which could be calculated in a straightforward way by knowing the weight of the polystyrene microspheres in 1 ml of suspension, the size of the microspheres, and the density of polystyrene. This permitted calculation of the (maximum) scattering coefficient  $\mu_s$  of each polystyrene suspension used. Since dilution of the manufacturer shipped solutions to produce any phantom in a series resulted in a corresponding decrease of the number density of spheres per unit volume, the scattering coefficient at any dilution could be obtained easily from the scattering coefficient of the manufacturer shipped solutions upon multiplying it by the appropriate volume fraction,  $f$ , of the microspheres in the phantom. For example, the extinction cross section for the 0.5  $\mu\text{m}$  microspheres (refractive index 1.6) in water (refractive index 1.33) from the Van de Hulst approximation at  $\lambda = 337 \text{ nm}$  (using Equation 8 from reference [7]) was  $C_{\text{ext}} = 4.4 \times 10^{-9} \text{ cm}^2$ . The number of 0.5 micron spheres in 1 ml of the manufacturer shipped suspension (containing 0.025 g of polystyrene per ml with polystyrene density 1.05 g/ml) was  $N_s = 3.6 \times 10^{11}$ , giving a maximum scattering coefficient  $\mu_s = 1584 \text{ cm}^{-1}$ . Thus, a phantom with microsphere volume fraction  $f = 0.1$  had a scattering coefficient of  $158 \text{ cm}^{-1}$  at  $\lambda = 337 \text{ nm}$ . The values of scattering coefficients calculated in this manner for all phantoms prepared were maintained at values similar to the reported optical scattering of biological tissues [43].

In order to determine whether there was any variation in the fluorophore lifetime resulting from potential variations in fluorophore concentration introduced via the use of micropipettes for successive phantom preparations in a series (as described above), a set of control dilutions were prepared with fluorescein by substituting the scattering suspension in the above steps with the solvent (DI H<sub>2</sub>O, in this case). The variations between the measured lifetimes in the control set were negligible (less than 3%), and therefore the data presented below do not use a control set. Samples were checked for potential artifacts introduced by photobleaching by preparing two phantom media with 0% scatterers (one for each dye) with the fluorophore concentration being equal to the highest dye concentration used in the prepared phantom-series for that fluorophore (40  $\mu\text{M}$ , fluorescein; 10  $\mu\text{M}$  IR-125). Each of these phantoms was illuminated for a period of five minutes and it was verified that there was no photobleaching (decrease in signal) in the samples at the end of that duration. Since the time to obtain three measurements from each phantom was well under one minute, the data are considered to be devoid of photobleaching effects.

### 2.3. Data Analysis

Time-resolved fluorescence data were collected for the phantom series indicated in Table 1. Data analysis methods have been described in detail previously [41]. In short, the measured time-resolved data ( $M(t)$ ) from each phantom is understood to be a convolution of the intrinsic fluorescence signal ( $F(t)$ ) with the instrument response ( $I(t)$ ):  $M(t) = F(t) * I(t)$ . For the phantom experiments presented here, the intrinsic fluorescence signal was taken to be a mono-exponential decay with characteristic lifetime  $\tau$ , i.e.  $F(t) \sim \exp(-t/\tau)$  [28, 41]. The instrument response function  $I(t)$  represents distortions in the detected time-resolved dynamics due to the response of the electronics, the optics, and the finite temporal profile of the excitation pulse. Both of the instruments required measurements of the instrument response function. The UV-FLS measured  $I(t)$  as the detected remitted fluorescence signal from a 1  $\mu\text{M}$  solution of Rose Bengal in DI water, which has a lifetime of  $\sim 90 \text{ ps}$  [44]

(below the temporal resolution of the UV-FLS [41]). The instrument response for the NIR-FLS was obtained by measuring the reflectance from a scattering solution (containing 1.0  $\mu\text{m}$  microspheres at volume fraction  $f = 0.1$ , with no fluorophore) using a band pass filter centered at  $780 \pm 10$  nm to select the excitation signal and the APD for detection. The measured fluorescence signal,  $M(t)$ , from a phantom was analyzed using a least-squares iterative reconvolution procedure based on the Marquardt algorithm (Light Analysis, Quantum Northwest, Inc. WA) to extract the best-fit lifetime  $\tau$  for the measurement [41].

For each phantom series in Table 1, the measured lifetime ratio  $\tau_0/\tau$  was plotted vs. polystyrene microsphere (quencher) concentration and these data were analyzed via the linear Stern-Volmer equation (Equation 1). (For all data, the plotted lifetime ratio represents the mean value of three measurements and the error bars reflect the standard deviation of these measurements for each phantom medium.) As described below, the microsphere (quencher) concentration can be expressed in multiple ways, leading to different numerical values for  $K_D$  (the Stern-Volmer quenching constant) with units that correspond to the units used for quencher concentration. Regardless of the exact units chosen to represent the quencher (microsphere) concentration, when the lifetime ratio for each phantom series was analyzed using the Stern-Volmer equation,  $K_D^{-1}$  represented the microsphere concentration at which 50% of the intrinsic dye fluorescence was quenched by the microspheres. Hence, the larger the Stern-Volmer quenching constant  $K_D$  was for a phantom series, the lesser the concentration of quencher (in that series) required to quench 50% of the fluorescence from the fluorescent dye, or, in other words, the more efficient was the quencher. It was observed that each phantom containing a non-zero microsphere (scatterer) concentration displayed a decreased (quenched) lifetime  $\tau$  relative to  $\tau_0$ . This reduction in lifetime was dependent on  $f$ , the volume fraction of the microspheres in the phantom, with the amount of quenching exhibited by each phantom in the series increasing linearly with  $f$  as  $\tau_0/\tau = 1 + K_f f$ , where the Stern-Volmer quenching constant  $K_D$  is denoted as  $K_f$ .

### 3. Results and Discussion

Fluorophore lifetimes for phantoms in each series listed in Table 1 were measured and these results are shown in Fig. 3-5. For each phantom-series, the lifetime measured for the phantom with 0% scatterers was taken to be the intrinsic lifetime of the fluorophore ( $\tau_0$ ).

Figure 3(a, b) shows the measured variation in fluorophore lifetimes relative to the intrinsic lifetime of fluorescein at 8  $\mu\text{M}$  ( $\tau_0 = 3.6$  ns) for phantom series-D (2.0  $\mu\text{m}$  microspheres, circles), series-E (1.0  $\mu\text{m}$  microspheres, triangles), and series-F (0.5  $\mu\text{m}$  microspheres, squares). Figure 3(a) shows the collisional quenching for each phantom in a series with the magnitude of quenching being proportional to the volume fraction  $f$  of the microspheres in the series. At  $f = 0.5$ , Series-D (2.0  $\mu\text{m}$  microspheres,  $K_f = 0.74$ ) showed a lifetime decrease of 35%, series E (1.0  $\mu\text{m}$  microspheres,  $K_f = 0.24$ ) showed a lifetime decrease of 10% and series F (0.5  $\mu\text{m}$  microspheres,  $K_f = 0.44$ ) showed a lifetime decrease of 20%. Thus, the fluorescence quenching observed in the presence of polystyrene microspheres increased with increasing microsphere concentration, suggesting that polystyrene microspheres provided a quencher-species that collisionally quenched the fluorescence from the dye.

Figure 3(a) expresses quencher concentration as the volume fraction of the microspheres in the phantom. Comparisons of relative quenching efficiencies between different sized microspheres may be facilitated by assuming that the polystyrene microspheres provide quenching sites residing on the surface of the spheres. Thus, the total number of quenching sites (which would determine the quencher concentration, physically) would be proportional to (i) the number density of the microspheres (number of microspheres per unit ml) in the phantom, and (ii) the total surface area of microspheres in the phantom (per unit ml of the

phantom). This suggests expressing the quencher concentration in units of the total microsphere surface area exposed per unit ml ( $\sigma$ ) of the phantom instead of the volume fraction of microspheres. The number density of the microspheres in a given phantom depends on both the volume fraction of the microspheres in the phantom and on the inverse third power of the microsphere diameter ( $\sim d^{-3}$ ), since each manufacturer shipped

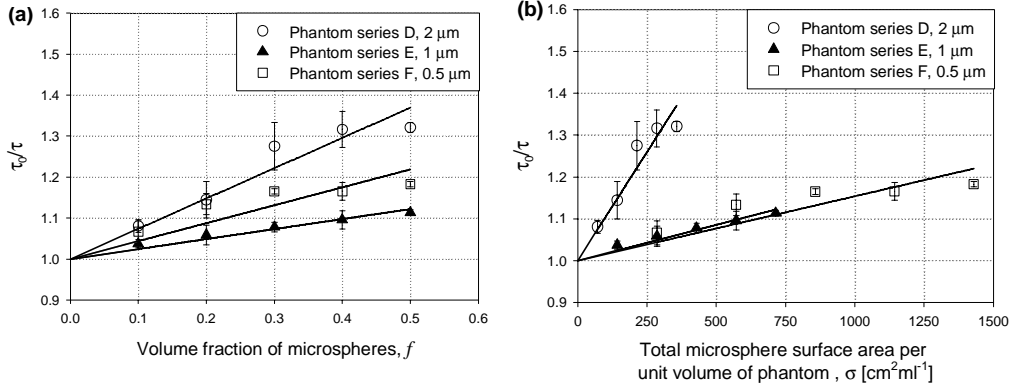


Fig. 3. (a) Measured variation in fluorophore lifetime  $\tau$  (relative to the intrinsic lifetime  $\tau_0$ ) at fixed fluorescein concentration of 8  $\mu\text{M}$  plotted vs. varying volume fractions of polystyrene microspheres, for three different sizes of the microspheres. (b) Same data as in (a), but now plotted vs.  $\sigma$ , the available surface area presented by the microspheres per unit ml of phantom media.

microsphere solution contained a constant weight of the microspheres suspended per unit volume (25 g/l). The presence of quenching sites on the surface of each microsphere would further scale the quencher concentration as the square of the microsphere sphere diameter ( $\sim d^2$ ). For example, the number of 0.5  $\mu\text{m}$  microspheres per unit ml in the manufacturer shipped suspension was  $N_s = 3.6 \times 10^{11}$ . Therefore in a phantom containing 0.5  $\mu\text{m}$  microspheres at a volume fraction of  $f = 0.5$ , the total microsphere surface area exposed per unit ml  $\sigma = N_s f \pi d^2$  (where  $d$  is the diameter of the microspheres in cm), leading to  $\sigma = 1420 \text{ cm}^2\text{ml}^{-1}$ . Thus, the Stern-Volmer quenching constant may be written as  $K_\sigma$  if calculated for each phantom series by expressing the quencher (microsphere) concentration in terms of  $\sigma$ .

Figure 3(b) shows the data in Fig. 3(a) plotted against available surface area  $\sigma$  (in  $\text{cm}^2$ ) on the microspheres per unit ml of the phantom media (as described above). In scaling the quencher concentration from microsphere volume fraction  $f$  to the available surface area per ml  $\sigma$  of phantom, the data from series E and F ( $K_\sigma = 1.7 \times 10^{-4}$  and  $1.5 \times 10^{-4} \text{ mlcm}^{-2}$ , respectively) become nearly collinear, suggesting that quenching mechanisms arising from the 1.0  $\mu\text{m}$  or the 0.5  $\mu\text{m}$  diameter microspheres might be similar in origin and dependent on the surface area of the microspheres. Further, since the quenching efficiency of phantom series D ( $K_\sigma = 10.0 \times 10^{-4} \text{ mlcm}^{-2}$ ) is much greater than that exhibited by either series E or F, the data suggest the possibility that quenching differences occurring in the 2.0  $\mu\text{m}$  microspheres could be related to the fabrication of the larger spheres. According to the manufacturer, polystyrene microspheres are fabricated by an emulsion polymerization process, which makes the microspheres more akin to a ball of wool than a hard sphere. The manufacturer also reported that the microspheres do not contain any surfactant but carry a slight anionic charge on their surface and that for some fluorescently labeled microspheres the dye resides on the outer 10% of the sphere volume. The behavior described above for phantom series D, E, and F was identical to that observed in phantom series A, B, and C (data not shown).

Figure 4 shows variation of fluorophore lifetimes for two phantom series with differing fluorophore concentrations: series A with 40  $\mu\text{M}$  fluorescein ( $\tau_0 = 3.9 \text{ ns}$ ,  $K_\sigma = 6.0 \times 10^{-4} \text{ mlcm}^{-2}$ ) and series D with 8  $\mu\text{M}$  fluorescein. Both these series used microspheres of diameter 2.0  $\mu\text{m}$  as the quencher. It can be seen that the phantom series with higher dye concentration displayed a decreased quenching efficiency relative to the series with lower dye

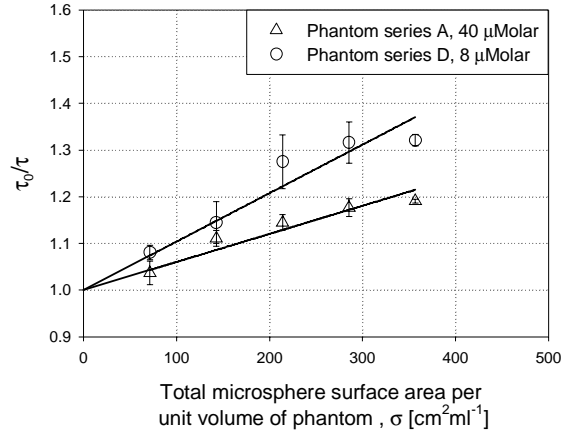


Fig. 4. Measured variation in fluorophore lifetime  $\tau$  (relative to the intrinsic lifetime  $\tau_0$ ) plotted vs.  $\sigma$ , the available surface area presented by the polystyrene microspheres per unit ml of phantom media, for two phantom series at different fluorophore concentrations: series A (40  $\mu\text{M}$  fluorescein, triangles) and series D (8  $\mu\text{M}$  fluorescein, circles). Both phantom series contained 2.0  $\mu\text{m}$  diameter microspheres. For the highest microsphere concentration, phantom series A showed a 20% decrease in measured lifetime, while series D showed up to a 30% decrease for the same microsphere concentration.

concentration.

Similarly, Fig. 5 shows the observed lifetime quenching of IR-125 dye with increasing quencher (2.0  $\mu\text{m}$  microsphere) concentration, at two differing dye concentrations. The dye concentration was held at 1  $\mu\text{M}$  IR-125 in series G ( $\tau_0 = 0.6 \text{ ns}$ ,  $K_\sigma = 11.0 \times 10^{-4} \text{ mlcm}^{-2}$ ) and 10  $\mu\text{M}$  IR-125 in series H ( $\tau_0 = 0.4 \text{ ns}$ ,  $K_\sigma = 6.5 \times 10^{-4} \text{ mlcm}^{-2}$ ). As in the case of fluorescein (series A and D), the IR-125 series with higher dye concentration displayed a decrease in quenching efficiency relative to the IR-125 series with lower dye concentration, at identical volume fractions of the same microsphere in both series. Series G showed a decrease of 20% in lifetime when the surface area of the microspheres per unit ml  $\sigma = 200 \text{ cm}^2\text{ml}^{-1}$ , while series H showed the same decrease in lifetime when the surface area of the microspheres per unit ml  $\sigma = 350 \text{ cm}^2\text{ml}^{-1}$ .

It is seen from Fig. 4 and 5 that increasing the dye concentration decreased the quenching efficiency. This may be understood physically by considering that collisional quenching phenomena arise only when dye molecules come into contact with the quenching agent, which in turn is taken to be present on the surface of the polystyrene microspheres. Hence, only dye molecules that are within some spatial proximity to a microsphere will be affected by the quenching phenomenon. Thus, if there are a relatively greater number (higher concentration) of dye molecules outside the “quenching field” of the microspheres, on average, then the fraction of quenched dye molecules will be lesser in that phantom, leading to an apparent decreased quenching effect, as observed, relative to lower dye concentrations. Preparing tissue-simulating phantoms using higher dye concentrations may reduce the effects

of collisional quenching, but these samples should be carefully checked for other quenching artifacts arising from reabsorption (inner filter) effects at these higher concentrations [38].

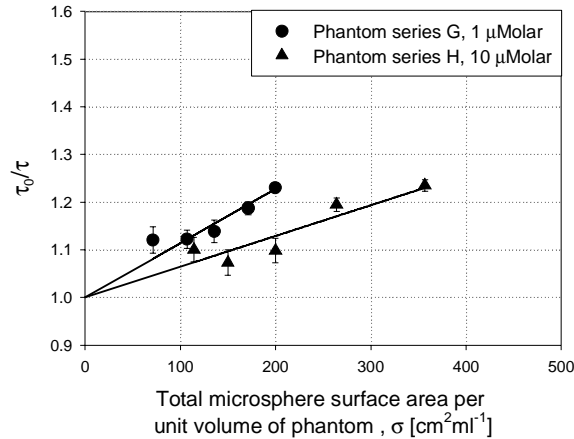


Fig. 5. Measured variation in fluorophore lifetime  $\tau$  (relative to the intrinsic lifetime  $\tau_0$ ) plotted vs.  $\sigma$ , the available surface area presented by the polystyrene microspheres per unit ml of phantom media, for two phantom series at different fluorophore concentrations: series H (10  $\mu\text{M}$  IR-125, triangles) and series G (1  $\mu\text{M}$  IR-125, circles). Both phantom series contained 2.0  $\mu\text{m}$  diameter microspheres. These data for IR-125 reveal the same quenching behavior vs. fluorophore concentration as data in Fig. 4 for fluorescein.

In a previous study, the addition of polystyrene microspheres to create fluorescent tissue phantoms using three different laser dyes - 3,3'-diethylthiatricarbocyanine iodide (DTTCl), IR-125, and IR-140 - indicated that the fluorophore lifetimes decreased by approximately 20%, 7% and 18%, respectively, relative to lifetimes obtained in the absence of microspheres from the same dye solutions [28]. This previous study suggested that these lifetime decreases might be attributed to varying amounts of water in the polystyrene microsphere suspensions used. The results presented here in this report suggest the possibility that collisional quenching by polystyrene microspheres might account for the decreases previously observed.

The results presented here indicate that polystyrene microspheres can act to collisionally quench the intrinsic fluorescence from both fluorescein and IR-125. The data shown in the figures (consisting of 6 measurements for fluorescein tissue phantoms and 2 measurements for IR-125 tissue phantoms) are representative of trends verified on 11 different fluorescein tissue phantoms and 4 different IR-125 tissue phantoms. Thus, using polystyrene microspheres to create fluorescent tissue-simulating phantoms in order to calibrate instrumentation or derive theoretical expressions for spatially (or temporally) resolved fluorescence may require monitoring for quenching effects that can occur in the phantom and skew the remitted fluorescence signal. For example, steady-state measurements of total remitted fluorescence vs. changing source-detector separations will be unaffected by quenching due to a normalization procedure employed in calculating the optical properties of the phantom [45, 46]. However, an experiment using fluorescent tissue phantoms to measure absolute intensity values would be affected by such quenching phenomena.

#### 4. Summary and Conclusions

Time-resolved fluorescence measurements were obtained from media containing a mixture of a fluorescent dye solution in a suspension of polystyrene microspheres. Fluorophore

lifetimes obtained from these measurements indicated that the presence of the polystyrene microspheres changed the intrinsic lifetime of the fluorophore via collisional quenching. The magnitudes of these quenching effects were quantified by using the equation (1) to extract the Stern-Volmer quenching constants and these results are summarized in Table 2. As described above, the value of the quenching constants depends on the units chosen to express the quencher concentrations and the uncertainty in the value of the quenching constant for each phantom series arises from the uncertainty in measurements of the intrinsic fluorophore lifetimes for that phantom series (denoted parenthetically in Table 2). For phantom series B-C and series D-E, expression of the quencher concentration in terms of  $\sigma$  (calculated as the total available microsphere surface area per unit ml of phantom) leads to near identical values for  $K_\sigma$  for the phantoms series B and C and series D and E.

Table 2. Summary of Stern-Volmer quenching constants for phantom series measured

Phantom Series	Intrinsic lifetime (ns), $\tau_0$ ( $\Delta\tau_0$ )	$K_f$ ( $\Delta K_f$ )	$K_\sigma$ ( $\Delta K_\sigma$ ) ( $\text{cm}^2\text{ml}^{-1}$ )
A	3.9 (0.2)	0.59(0.11)	0.83(0.16) $\times 10^{-3}$
B	3.9 (0.2)	0.18(0.10)	0.13(0.07) $\times 10^{-3}$
C	3.9 (0.2)	0.51(0.11)	0.17(0.04) $\times 10^{-3}$
D	3.6 (0.2)	0.84(0.14)	1.20(0.19) $\times 10^{-3}$
E	3.6 (0.2)	0.33(0.12)	0.20(0.08) $\times 10^{-3}$
F	3.6 (0.2)	0.52(0.12)	0.20(0.04) $\times 10^{-3}$
G	0.4 (0.1)	1.50(0.97)	2.01(0.70) $\times 10^{-3}$
H	0.6 (0.1)	0.74 (0.39)	1.02(0.50) $\times 10^{-3}$

Polystyrene microspheres are often employed to create turbid media having optical scattering properties similar to human tissue that can be used to quantify optical scattering via theoretical or experimental methods. Fluorescent tissue phantoms created using polystyrene microspheres to provide optical scattering may be subject to quenching of the intrinsic fluorescence, leading to a loss in remitted fluorescence and a reduced fluorophore lifetime. Since many tissue-simulating phantoms are used in studies that observe changes in remitted intensity, the quenching effects of polystyrene microspheres may be difficult to isolate unless fluorescence lifetime measurements are performed.

### Acknowledgments

The authors wish to thank Dr. P. Urayama for useful discussions and technical assistance. This work was supported in part by a grant from the National Institutes of Health CA-114542 (to M.-A.M.). M. Close was a student supported by the National Science Foundation's Research Experience for Undergraduates program in Molecular Materials at Dartmouth College DMR-9820408.